BENG 221: Problem Solving Project

Multiscale Model of Oxygen transport in Diabetes

December 1, 2016

Austin Burdick
Nafeesa Khan
Srihita Rudraraju

Motivation

Diabetes remains a significant health condition today, and affects not only key regulatory systems within the body, but certain bodily tissues as well. This disease is perhaps best associated with a disturbance in the processing of sugar consumed through food, due to either a lack of insulin or to a decreased efficiency of this hormone within an affected person[1]. However, it is equally important to note that diabetes has demonstrated effects within the composition of the microvasculature, shown by thickening of the basement membrane in human capillaries[2]. This alteration of the vessel structure can be linked to a deficiency in the amount of oxygen that is ultimately transported to the surrounding body tissue[3]. By modelling the physiological effects of diabetes on the capillaries, the effects of this disease can be better understood in order to potentially mitigate its accompanying health risks.

The scope of diabetes within the United States alone has been well established. The Centers for Disease Control and Prevention (CDC) have estimated that 29.1 million, or 9.3%, of the population have developed some form of diabetes, with approximately 8 million of this number remaining undiagnosed[4]. This condition has been related to other health risks as well, as death rates from cardiovascular disease have been shown to be almost twice as high in affected individuals over eighteen years old. Additionally, hospitalization rates for instances of both heart attack and stroke are almost twice as high in affected individuals over twenty years old. The effects of diabetes also include significant medical costs, with $176 billion, over two times the costs for those without this disease, estimated for average expenditures[4].

Problem Statement

Basement membrane thickening is a significant change affected by the development of diabetes in both type I and type II varieties. Because it is composed of proteins that are closely related to collagen, this membrane experiences an increase in protein synthesis when subjected to various types of damage caused by diabetes and its related health conditions[2]. This state of the vessel boundary, as pictured in Figure 1, has been linked to several conditions resulting from diabetes, such as neuropathy[3]. Additionally,

research[5] has yielded distributions of membrane thickness for both diabetic patients as well as unaffected individuals. The results, shown in Figure 2, display a significant increase in membrane width that is enhanced with age 5. Further studies have implied that this increase in thickness is due to a large turnover accompanied by a significant decrease in the eventual degradation of the membrane[2].

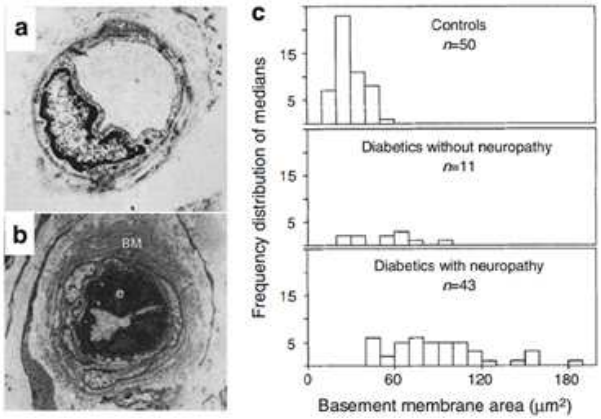

Figure 1: Images of capillaries with both normal and increased thickness (left) along with distributions of membrane area in normal and diabetic patients.[3]

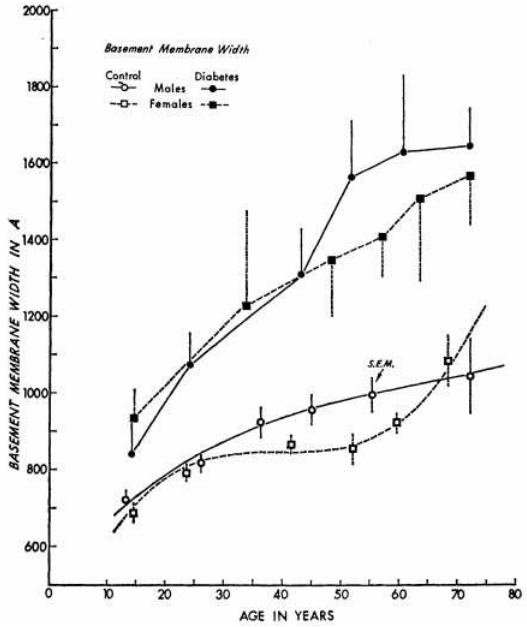

Figure 2: Effects of diabetes and aging on membrane thickness compared to unaffected individuals.[5]

The effects of diabetes on the capillary basement membrane width result in multiple disruptions in the final steps of oxygen delivery. After passing the vessel wall following release, diffusion is the primary driving force of oxygen to reach the surrounding tissue. However, the distance that can be covered by this process is extremely limited, requiring

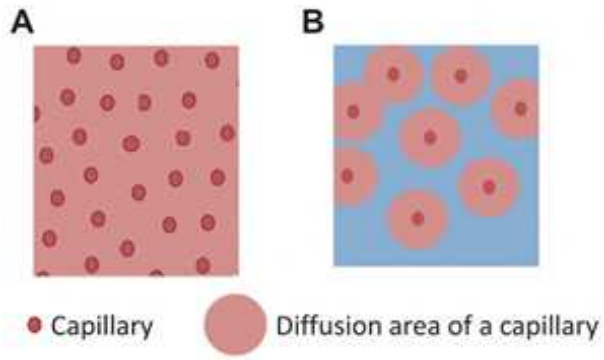

Figure 3: Oxygen transport under normal and diabetic conditions. Distance between the individual capillaries is increased, reducing the effects of normal diffusion.[7]

close arrangement of the capillary array. In patients with diabetes, the space between individual capillaries is greatly increased, while the limited range of diffusion creates regions in the tissue where ischemia can develop (Figure 3). In this case, therapies might be necessary in order to increase the partial pressure of oxygen within the vessels, restoring delivery[6].

Prior to diffusion outside the vessels, oxygen deficiency may also occur due to an increase in blood velocity due to diabetes. It has been reported that during an increase in membrane width, a "shunt" may occur within the vessel network, perturbing flow within the capillaries and preventing delivery to the surrounding tissue due to less time for oxygen extraction[3]. While this prompts an increase in blood flow to meet the needs of the tissue, hypoxia can arise in the adjacent cells[3]. This increase in fluid velocity has also been observed in other studies of diabetes, listing an interquartile range from 15.9 x 10^{-3} cm/s to 89.0 x 10^{-3} cm/s in those unaffected by diabetes, and a range from 68.4 x 10^{-3} cm/s to 21.8 x 10^{-2} cm/s in those with the condition[7].

Both the increase in distance between capillaries and the disturbed flow within the vasculature provide the basis for a model that can represent the extent of diabetes with respect to oxygen delivery. In each case, the final transfer of oxygen to the body is inhibited, due to increases in the flow of the blood itself as well as to increased distances covered by the basement membrane. By taking the parameters found under each of these conditions into account, oxygen movement within the capillaries can be characterized at each step. This is modelled from the release of molecules from hemoglobin into an individual vessel, followed by passage through the surrounding wall and basement membrane, and finally through the tissue itself. In this way, the extent of change

to this process under diabetic conditions can be better understood by way of a comprehensive model.

Model

The model derived is based on oxygen transport at multiple stages within a vessel and its surrounding tissues. In this instance, movement through the vessel itself, the vessel wall, and a portion of tissue beyond the wall has been accounted for. The blood vessel is modeled as a single capillary where hemoglobin releases oxygen, which exits the cell as it enters into the plasma. From here, oxygen travels to the vessel wall, normally experiencing both convection and diffusion while moving towards a layer of endothelial cells, and subsequently diffusing further into the absorbing tissue (Figure 4).

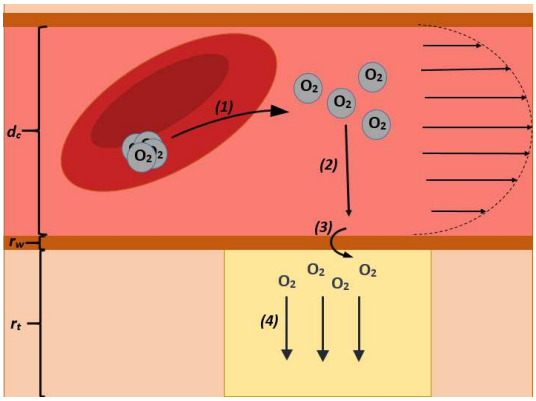

Figure 4: Model of oxygen transport within a single capillary. This pathway depicted indicates oxygen release from hemoglobin and exit from the cell, followed by flow down the vessel and diffusion to the vessel wall and surrounding tissue.

Within the developed model, certain assumptions are made to produce a mathematical analysis of oxygen transport. The interstitial space between the vessel wall and the tissue has been disregarded. Assumptions are determined for each stage of transport, and are made based on reasonable estimates as well as a focus on diffusion in a single dimension within the model. The following sections explain each stage in further detail.

Blood vessel

The assumptions considered for the blood vessel are listed below.

1) Homogenous solution of hemoglobin

2) No diffusion in the axial direction

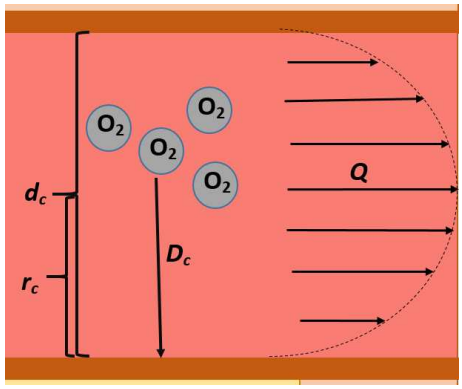

Figure 5: Model of oxygen transport within a blood capillary.

3) No flow in the radial direction

4) Hb, HbO_2 and O_2 are in equilibrium

5) Constant velocity of oxygen along the axial (z) direction

6) Constant diffusion coefficient D_c

Convection currents are not important for our model and transport of oxygen occurs primarily in the radial direction. Considering these simplifications, the blood vessel is modeled as a small capillary[10]. Diffusion occurs exclusively in the radial direction at a constant diffusivity D_c and axial diffusion is ignored. Deoxygenated hemoglobin and oxygen are assumed to be in equilibrium with oxygenated hemoglobin, and the concentration of hemoglobin [Hb] is held constant. Finally, the velocity of oxygen transported is only considered in the z-direction at a constant rate v. From these parameters, the following balance equations are utilized for hemoglobin and oxygen.

$$\frac{\partial[O_2]}{\partial t} + v.\nabla[O_2] = D_{O_2}\nabla^2[O_2] - R_{O_2} \tag{1}$$

$$\frac{\partial[HbO_2]}{\partial t} + v.\nabla[HbO_2] = D_{HbO_2}\nabla^2[HbO_2] - R_{O_2} \tag{2}$$

These equations are simplified for the case of steady state flow and oxygen transport in a cylindrical conduit. Considering neglected diffusion in axial (z), or flow direction and no flow in the radial direction (r), the equations are translated to as below.

$$v\frac{\partial[O_2]}{\partial z} = D_{O_2}(\frac{\partial^2[O_2]}{\partial r^2} + \frac{1}{r}\frac{\partial[O_2]}{\partial r}) - k^{'}[Hb][O_2] + k[HbO_2] \tag{3}$$

$$v\frac{\partial[HbO_2]}{\partial z} = D_{HbO_2}(\frac{\partial^2[HbO_2]}{\partial r^2} + \frac{1}{r}\frac{\partial[HbO_2]}{\partial r}) + k^{'}[Hb][O_2] - k[HbO_2] \quad (4)$$

In order to obtain the analytical solution, the problem is further simplified. Fluid velocity is only considered in the radial direction, oxyhemoglobin and oxygen are in local chemical equilibrium (or the rate of reaction is zero), and diffusion only in the radial direction. No net oxygen exchange was assumed across the boundary. Thus, zero flux boundary conditions are considered at both boundaries of capillary. The initial concentration of oxygen in the capillary is modeled on the basis of fluid velocity inside a tube. Consequently, the concentration is highest at the center of the capillary C_0 and is zero at the boundary, varying radially in a linear fashion. The above assumptions lead to the following equation.

$$\frac{\partial[O_2]}{\partial t} = \frac{D_c}{r}\frac{\partial(r\frac{\partial[O_2]}{\partial r})}{\partial r} \quad (5)$$

Boundary conditions:

$$\frac{\partial[O_2]}{\partial r}(0,t) = 0 \qquad \frac{\partial[O_2]}{\partial t}(r_{cw},t) = 0 \quad (6)$$

Initial condition:

$$[O_2](r,0) = C_0(1 - \frac{r}{r_{cw}}) \quad (7)$$

Vessel wall

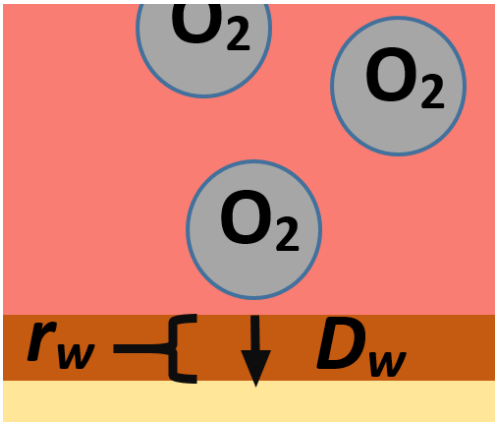

Figure 6: Model of oxygen transport within the vessel wall.

The assumptions for this stage are as follows:

- Diffusion only occurs in the radial direction

- Uniform consumption of oxygen by mitochondria in endothelial cells

- Constant diffusivity D_w

Similar assumptions as the capillary are made for the vessel wall. Additionally, a constant consumption term of oxygen by mitochondria is considered. This consumption term is represented as M_w. A simple way of connecting the three stages of oxygen transport is devised. The steady state value of oxygen concentration is used as a boundary condition for the consequent stage. Thus, steady state oxygen concentration derived from the capillary stage is used as a boundary condition here. Zero flux condition is considered at the other boundary. It is also assumed that there is no oxygen present in the vessel wall initially. These assumptions lead to the following equations.

$$\frac{\partial [O_2]}{\partial t} = \frac{D_w}{r} \frac{\partial (r \frac{\partial [O_2]}{\partial r})}{\partial r} - M_w \tag{8}$$

Boundary conditions:

$$[O_2](r_{cw}, t) = C_0 - 0.5 \qquad \frac{\partial [O_2]}{\partial t}(r_{wt}, t) = 0 \tag{9}$$

Initial condition:

$$[O_2](r, 0) = 0 \tag{10}$$

Tissue

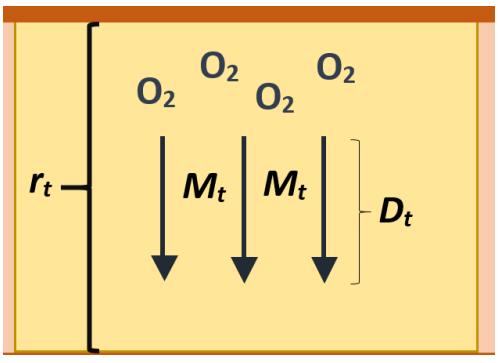

Figure 7: Model of oxygen transport within the surrounding tissue.

The assumptions considered for the surrounding tissue are as given:

- Diffusion only occurs in the radial direction

- Uniform consumption of oxygen by mitochondria in endothelial cells

- Constant diffusivity D_t

Assumptions for the surrounding tissue are similar to those considered in the vessel wall. Steady state oxygen concentration in the vessel wall is used as a boundary condition here. It is assumed that there is no oxygen present in the tissue initially. The equations are as follows.

$$\frac{\partial[O_2]}{\partial t} = \frac{D_t}{r}\frac{\partial(r\frac{\partial[O_2]}{\partial r})}{\partial r} - M_t \tag{11}$$

Boundary conditions:

$$[O_2](r_{wt}, t) = \frac{M_w}{4D_w}r_{wt}^2 + C_0 - 0.5 \qquad \frac{\partial[O_2]}{\partial t}(r_t, t) = 0 \tag{12}$$

Initial condition:

$$[O_2](r, 0) = 0 \tag{13}$$

Analytical Solution

Blood vessel

$$\frac{\partial[O_2]}{\partial t} = \frac{D_c}{r}\frac{\partial(r\frac{\partial[O_2]}{\partial r})}{\partial r} \tag{14}$$

Boundary conditions:

$$\frac{\partial[O_2]}{\partial r}(0, t) = 0 \qquad \frac{\partial[O_2]}{\partial t}(r_{cw}, t) = 0 \tag{15}$$

Initial condition:

$$[O_2](r, 0) = C_0(1 - \frac{r}{r_{cw}}) \tag{16}$$

This simplified model resembles a homogenous partial diffusion equation in the cylindrical coordinates. It can be solved using separation of variables.

$$u(r, t) = X(r)T(t) \tag{17}$$

Substituting this new definition into the homogenous PDE and rearranging results in one time-dependent equation and one space-dependent equation. Bessel functions are

used for the solution.

$$T(t) = Ce^{-D\lambda^2 t} \tag{18}$$

$$r^2\frac{\partial^2 X}{\partial r^2} + r\frac{\partial X}{\partial r} + r^2\lambda^2 x = 0 \tag{19}$$

$$X(r) = AJ_0(\lambda r) \tag{20}$$

Applying the boundary conditions and using local extremes of Bessel function

$$\frac{\partial J_n(0)}{\partial r} = 0 \qquad \frac{\partial J_n(0)}{\partial r} = 0 \tag{21}$$

$$X = \lambda_{n_0} r \tag{22}$$

Using the principle of superposition, the final solution to the homogenous equation is the weighted sum of all possible solutions:

$$u(r,t) = \sum_{n=1}^{\infty} A_n J_0(\lambda_n r)e^{-D\lambda^2 t} \tag{23}$$

To solve for the constant A_n, the initial condition is applied to the above solution. The result is integrated over the radius of the capillary.

$$u(r,0) = u_0(r) = \sum_{n=1}^{\infty} A_n J_0(\lambda_n r) \tag{24}$$

$$\int_0^{r_{cw}} u_0(r)J_0(\lambda_m r)rdr = \sum_{n=1}^{\infty} A_n \int_0^{r_{cw}} J_0(\lambda_n r)J_0(\lambda_m r)rdr \tag{25}$$

$$\int_0^{r_{cw}} u_0(r)J_0(\lambda_m r)rdr = A_m\frac{r_{cw}^2}{2}J_1(\lambda_m r_{cw})^2 \tag{26}$$

$$A_m = \frac{2C_0\int_0^{r_{cw}}(1-\frac{r}{r_{cw}})J_0(\lambda_m r)rdr}{r_{cw}^2 J_1(\lambda_m r_{cw})^2} \tag{27}$$

Solving for integrals of the above Bessel functions becomes complicated. Hence, the

same setup is solved in Cartesian coordinates. The solution is as follows.

$$O_2(r,t) = (C_0 - 0.5) + \sum_{n=1}^{\infty} \frac{2C_0}{(n\pi)^2}(1 - cos(n\pi))cos(\frac{n\pi}{r_{cw}})e^{-D_c(\frac{}{2}n\pi r_{cw})t} \tag{28}$$

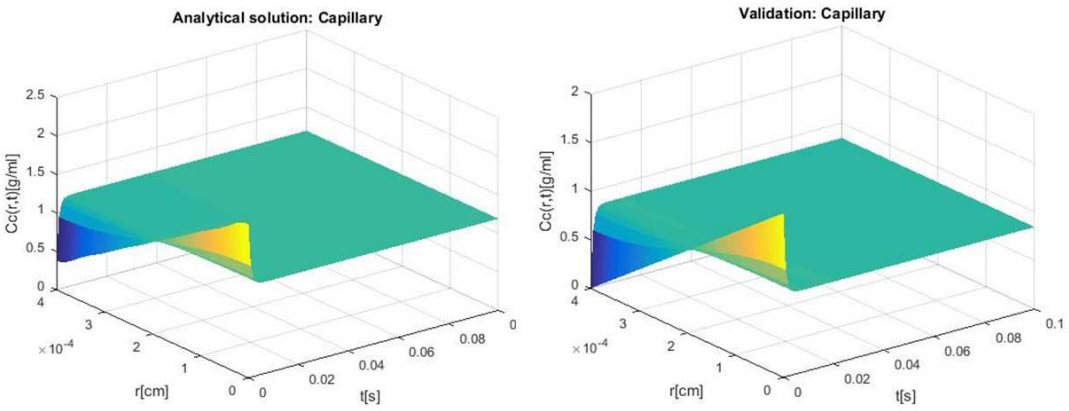

Figure 8: Analytical and numerical solution for blood vessel modeled as capillary in Cartesian coordinates.

Vessel wall

$$\frac{\partial[O_2]}{\partial t} = \frac{D_w}{r}\frac{\partial(r\frac{\partial[O_2]}{\partial r})}{\partial r} - M_w \tag{29}$$

Boundary conditions:

$$[O_2](0,t) = C_0 - 0.5 \qquad \frac{\partial[O_2]}{\partial t}(L_w,t) = 0 \tag{30}$$

Initial condition:

$$[O_2](r,0) = 0 \tag{31}$$

For the particular solution, a steady state condition was assumed to arrive at the solution.

$$0 = \frac{D_w}{r}\frac{\partial(r\frac{\partial[O_2]}{\partial r})}{\partial r} - M_w \tag{32}$$

$$u_p(r,t) = \frac{M_w}{4D_w}r^2 + C_0 - 0.5 \tag{33}$$

The homogenous partial diffusion equation in cylindrical coordinates can be solved using separation of variables.

$$u_h(r,t) = X(r)T(t) \tag{34}$$

Substituting this new definition into the homogenous PDE and rearranging results in one time-dependent equation and one space-dependent equation. Bessel functions are used for the solution.

$$T(t) = Ce^{-D\lambda^2 t} \tag{35}$$

$$r^2\frac{\partial^2 X}{\partial r^2} + r\frac{\partial X}{\partial r} + r^2\lambda^2 x = 0 \tag{36}$$

$$X(r) = AJ_0(\lambda r) \tag{37}$$

Applying the boundary conditions and using local extremes of Bessel function

$$\frac{\partial J_n(0)}{\partial r} = 0 \qquad \frac{\partial J_n(0)}{\partial r} = 0 \tag{38}$$

$$X = \lambda_{n_0} r \tag{39}$$

Using the principle of superposition, the final solution to the homogenous equation is the weighted sum of all possible solutions:

$$u_h(r,t) = \sum_{n=1}^{\infty} A_n J_0(\lambda_n r)e^{-D\lambda^2 t} \tag{40}$$

To solve for the constant A_n, the initial condition is applied to the sum of particular and homogenous solution. The result is integrated over the width of vessel wall.

$$u(r,0) = u_0(r) = \sum_{n=1}^{\infty} A_n J_0(\lambda_n r) \tag{41}$$

$$-\int_0^{L_w} u_0(r)J_0(\lambda_m r)rdr = \sum_{n=1}^{\infty} A_n \int_0^{L_w} J_0(\lambda_n r)J_0(\lambda_m r)rdr \tag{42}$$

$$-\int_0^{L_w} u_0(r)J_0(\lambda_m r)rdr = A_m \frac{r_{cw}^2}{2} J_1(\lambda_m L_w)^2 \tag{43}$$

$$u(r,t) = \sum_{n=1}^{\infty} -\frac{2}{L_w^2}\left(\frac{J_2(\lambda_m L_w - J_3(\lambda_m L_w))}{\lambda_m J_1(\lambda_m L_w)} + (C_0 - 0.5)L_w \frac{1}{\lambda J_1(\lambda_m L_w)}\right) J_0(\lambda_m L_w) e^{-D_w \lambda_m t} \tag{44}$$

Tissue

$$\frac{\partial [O_2]}{\partial t} = \frac{D_t}{r}\frac{\partial (r \frac{\partial [O_2]}{\partial r})}{\partial r} - M_t \tag{45}$$

Boundary conditions:

$$[O_2](0,t) = \frac{M_w}{4D_w} r_{cw}^2 + C_0 - 0.5 \qquad \frac{\partial [O_2]}{\partial t}(L_t, t) = 0 \tag{46}$$

Initial condition:

$$[O_2](r,0) = 0 \tag{47}$$

For the particular solution, a steady state condition was assumed to arrive at the solution.

$$0 = \frac{D_t}{r}\frac{\partial (r \frac{\partial [O_2]}{\partial r})}{\partial r} - M_t \tag{48}$$

$$u_p(r,t) = \frac{M_t}{4D_t} r^2 + C_0 - 0.5 \tag{49}$$

The solution is similar to that of vessel wall.

$$u(r,t) = \sum_{n=1}^{\infty} -\frac{2}{L_t^2}\left(\frac{J_2(\lambda_m L_t - J_3(\lambda_m L_t))}{\lambda_m J_1(\lambda_m L_t)} + \left(\frac{M_w}{4D_w} r_{wt}^2 + C_0 - 0.5\right)L_t \frac{1}{\lambda J_1(\lambda_m L_t)}\right) J_0(\lambda_m L_t) e^{-D_t \lambda_m t} \tag{50}$$

Table 1: Values of Parameters

Constant	*Description*	*Value*
v	O_2 velocity in capillary	0.1 cm/s[10]
v_d	O_2 velocity in capillary in diabetes	0.12 cm/s[7]
C_o	Initial O_2 concentration in capillary	1.62 x 10^{-4} g/ml[10]
[Hb]	Deoxyhemoglobin Concentration in capillary	0.55 g/ml[10]
[HbO_2]	Hemoglobin Concentration in capillary	0.34 g/ml[10]
k_p	Oxygen and Hemoglobin association rate	30 x 10^{-6} /Ms[11]
k	Oxygen dissociation rate	20 x 10^{-6} /Ms[11]
D_c	Diffusivity of O_2 in capillary	1.62 x 10^{-5} cm^2/s[10]
D_w	Diffusivity of O_2 in vessel wall	8.73 x 10^{-6} cm^2/s[10]
D_t	Diffusivity of O_2 in tissue	2.41 x 10^{-5} cm^2/s[10]
r_{cw}	Inner radius of vessel wall	4.0 x 10^{-4} cm[10]
r_{wt}	Outer radius of vessel wall	6.0 x 10^{-4} cm[8]
$r_{wt,d}$	Outer radius of vessel wall in diabetes	9.0 x 10^{-4} cm[8]
r_t	Outer radius of tissue	15.0 x 10^{-4} cm (arbitrary)
M_w	O_2 consumption in vessel wall	5.0 x 10^{-3} mlO_2/ml/s[12]
M_t	O_2 consumption in tissue	1.58 x 10^{-4} mlO_2/ml/s[12]

Numerical Model

The numerical validation is computed using MATLAB and its built-in PDE solver. Additional factors not included in the analytical solution are accounted for including: velocity of blood flow in the z-direction, dissociation rates of hemoglobin and oxygen, and coupling of boundary conditions between the different sections of the model. The equations used for the numerical validation are as follows and parameters are those listed in the table. Boundary and initial conditions mentioned in the model description have been used.

Blood vessel:

$$v\frac{\partial[O_2]}{\partial z} = D_c(\frac{\partial^2[O_2]}{\partial r^2} + \frac{1}{r}\frac{\partial[O_2]}{\partial r}) + R_{O_2} \tag{51}$$

$$R_{O_2} = k[HbO_2] - k_p[Hb][O_2] \tag{52}$$

Vessel wall:

$$\frac{\partial[O_2]}{\partial t} = \frac{D_w}{r}\frac{\partial(r\frac{\partial[O_2]}{\partial r})}{\partial r} - M_w \tag{53}$$

Surrounding tissue:

$$\frac{\partial[O_2]}{\partial t} = \frac{D_t}{r}\frac{\partial(r\frac{\partial[O_2]}{\partial r})}{\partial r} - M_t \tag{54}$$

In diabetic patients, the width of the vessel wall is larger compared to healthy condition. The following graphs illustrate the levels of oxygen concentration in diabetic condition in comparison to normal vessel wall width. In order to better visualize the oxygen concentration differences between diseased and healthy conditions, 2D graphs were plotted representing oxygen levels in each stage.

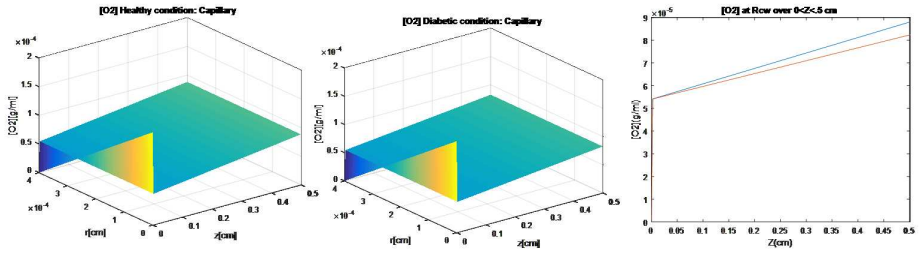

Figure 9: Plots of oxygen transport within healthy and diabetic capillaries.

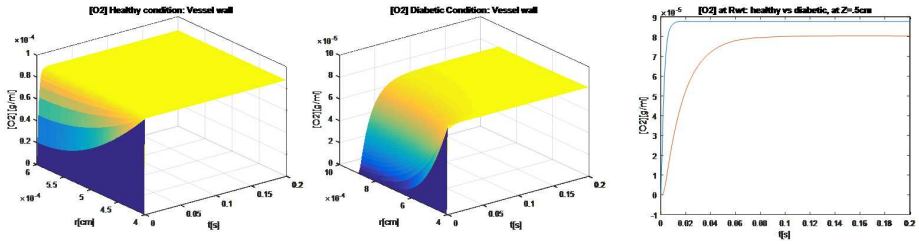

Figure 10: Plots of oxygen transport through the vessel wall under normal and diabetic conditions.

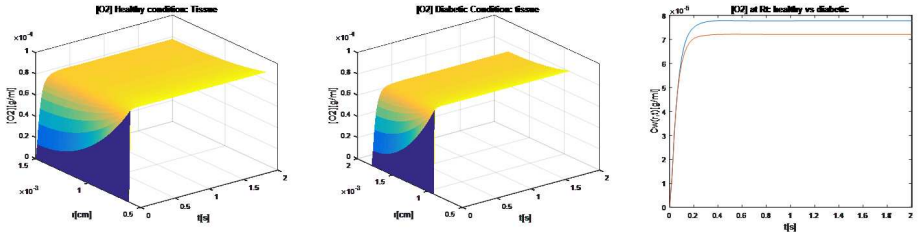

Figure 11: Plots of oxygen transport through the surrounding tissue under normal and diabetic conditions.

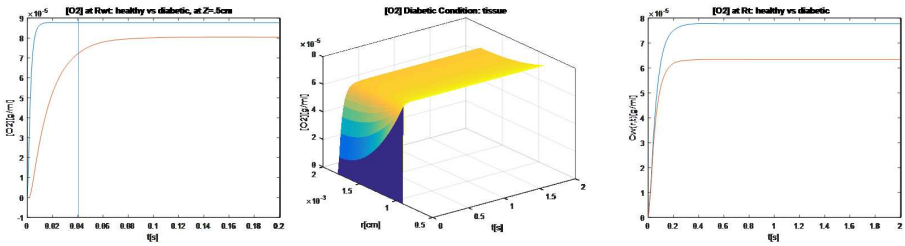

Figure 12: Oxygen transport cutoff within healthy and diabetic tissue at 0.4 seconds.

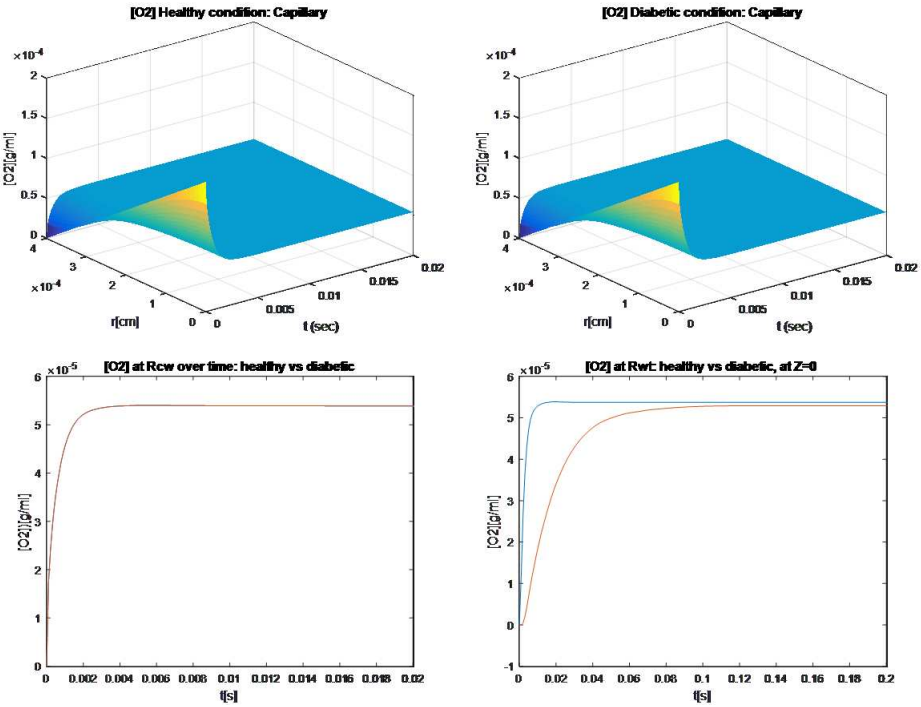

Figure 13: Oxygen transport within the capillary. Plots indicate the transport over time.

Conclusion and Future Work

We constructed a multi-scale model of oxygen diffusion from a capillary into surrounding tissue to show the effects of diabetes on oxygen availability. In the analytical model we simplified the both geometry and different stages involved in the process in addition to utilizing steady state solutions as boundary conditions for the following step in the transport of oxygen to the surrounding tissue. The effect of velocity increase in the diabetic condition on oxygen availability can be seen in the capillary plots of figure one. Increased velocity (by approximately 120%) in diabetes does not decrease the amount of oxygen available at the red blood cell (RBC) site (Z= 0 cm) (seen in figure 13 and plot 3 of figure 9) but does decrease the amount of oxygen further away (in our case Z= 0.5cm, figure 9 plot 3).

This difference in oxygen is carried through to the vessel wall and tissue (figures 10 and 11). The steady state value of the previous stage was taken as the left boundary condition in these calculations. As can be seen, the original difference in oxygen caused by velocity increase in diabetes carries through to the tissue. However, it is notable that the shape of the oxygen availability curve at the interface of the vessel wall and tissue (the third plot of figure 10), changes due to a thicker membrane.

Figure 12 shows the compounded effect of capillary membrane thickening and increased velocity, where a cutoff time is set at .04 seconds of diffusion in the vessel wall and is used as the left boundary condition in the tissue stage. This reflects that oxygen release by RBCs would come in pulses and diffusion would not go to steady state. In that case, the thicker membrane in addition to increased capillary velocity decreases the amount of oxygen available to tissue.

Finally, figure 13 shows the isolated effect of wall thickening on oxygen availability. Plots one through three demonstrate that even with velocity being higher in the diabetic condition, oxygen concentration is still the same at Z=0 (site of the RBC. However, even if the same amount of oxygen is available to the vessel wall between the healthy and diabetic case, the increased thickness still reduces oxygen availability (seen by the gap between the red and blue line in the fourth plot.

In the numerical model, we were able to account for more factors involved in the oxygen transport process and showed a decrease in the oxygen available to tissues during

diabetes by using literature-based changes in blood velocity and wall thickness. Consequently, less oxygen is available in the second step during transport through the capillary wall, where another confounding factor in diabetes, basement membrane thickening, further reduces the amount of oxygen that reaches the tissue. The difference in oxygen available to tissue at interfaces of the stages and at the end can be seen in figures one through three. Effectively, in the diabetic condition, oxygen is moving too quickly in the capillary to properly diffuse to the rest of the body, which is further hindered by a greater distance within the vessel wall that must be passed before reaching the tissue.

Chronic reduction in oxygen supply could be either correlative or causative with diabetes symptoms and complications. A primary argument for this would be a change in cell metabolism in response to decreased oxygen. Ostergaard et al. observed an increase in neuropathy in diabetic patients due to these changes in blood flow, which limited not only oxygen availability to tissue but glucose as well3. While we applied this model to the case of diabetes, it could also be used to analyze other disease states, such as anemia or sickle cell disease. In addition, modifications could be made to model transport of other nutrients or molecules, such as glucose, CO_2 or CO.

Multiple complex chemical, geometric and anatomical aspects of oxygen transport were either not included or were simplified for this model. These included assumptions regarding the nature of blood flow, simplifications in oxygen and hemoglobin dissociation kinetics, and simplified anatomy of the capillary (the interstitial space was not included). In order to build a more realistic model we would want to account for these aspects as well as the discrete nature of oxygen diffusion from individual red blood cells, instead of a continuum.

Our model shows the decrease in oxygen made available to tissue in the diabetic case compared to the healthy model. This is due to the observed increase in blood velocity through capillaries in diabetes as well as basement membrane thickening. Therefore oxygen has less time to diffuse through a given section of the capillary wall, and must also travel a greater distance before reaching the tissue. We believe that by taking this step to understanding the mechanisms of this disease, we provide a basis for continued research into more effective therapeutics for those affected. We hope to continue this study to gain further insight into increasingly complex scenarios provided by diabetes.

References

[1] Kelly, Jane. "Diabetes." *Centers for Disease Control and Prevention*, 2016. Accessed 24, Oct. 2016.

[2] Williamson, J.R., and C. Kilo. "Capillary Basement Membrane in Diabetes." *Diabetes* vol. 32, no. 2, 1983, pp. 96-100. Accessed 26, Oct. 2016.

[3] Ostergaard, Leif et al. "The effects of capillary dysfunction on oxygen and glucose extraction in diabetic neuropathy." *Diabetologia*, 2014, pp. 666-77. Accessed 26, Oct. 2016.

[4] "National Diabetes Report, 2014." *Centers for Disease Control and Prevention*, 2014. Accessed 27, Oct. 2016.

[5] Kilo, Charles, Nancy Vogler, and Joseph R. Williamson. "Muscle Capillary Basement Membrane Changes Related to Aging and to Diabetes Mellitus." *Departments of Medicine and Pathology, Washington University School of Medicine*, 1972, pp. 881-905. Accessed 25, Oct. 2016.

[6] Boulton, Andrew J. "The Diabetic Foot, an Issue of Medical Clinics." *Medical Clinics of North America*, vol. 97, no. 5, 2013, pp. 959-60. Accessed 24, Oct. 2016.

[7] Flynn, M.D., M.E. Edmonds, J.E. Tooke, and P.J. Watkins. "Direct measurement of capillary blood flow in the diabetic neuropathic foot" *Diabetologia*, 1989. Accessed 27, Oct. 2016.

[8] Hellums, J. David, et al. "Simulation of intraluminal gas transport processes in the microcirculation." *Annals of biomedical engineering* 24.1 (1995): 1-24.

[9] Vadapalli, Arjun, Roland N. Pittman, and Aleksander S. Popel. "Estimating oxygen transport resistance of the microvascular wall." *American Journal of Physiology-Heart and Circulatory Physiology* 279.2 (2000): H657-H671.

[10] Vadapalli, Arjun, Daniel Goldman, and Aleksander S. Popel. "Calculations of oxygen transport by red blood cells and hemoglobin solutions in capillaries." *Artificial Cells, Blood Substitutes, and Biotechnology* 30.3 (2002): 157-188.

[11] Vandegriff, K. D., et al. "Determination of the rate and equilibrium constants for oxygen and carbon monoxide binding to R-state human hemoglobin cross-linked between the alpha subunits at lysine 99." *Journal of Biological Chemistry* 266.26 (1991): 17049-17059.